Supplementary Information for

Edaphic specialization onto bare, rocky outcrops as a factor in the evolution of desert angiosperms

Isaac H. Lichter-Marck[a,b,*], & Bruce G. Baldwin,[a]

[a]Department of Integrative Biology and Jepson Herbarium, University of California Berkeley.
[2]Department of Ecology and Evolutionary Biology, University of California Los Angeles.

[*] Isaac H. Lichter-Marck

Email: ilichtermarck@berkeley.edu

This PDF file includes:

Supplementary text
Figures S1 to S8
Table S1 to S2
SI References

Supplemental Materials and Methods

Sampling, sequencing, phylogenetic inference, and divergence time estimation (DTE).

Our study included near-comprehensive coverage of all minimum-rank taxa of tribe Perityleae except *Pericome macrocephala* B.L. Rob., *Perityle aurea* Rose, *Laphamia grandifolia* (Brandegee) I.H. Lichter-Marck, *L. warnockii* (A.M. Powell) I.H. Lichter-Marck, and the four taxa of genus *Villanova* Lag. in subtribe Galeaninae for which material was unattainable. Three additional taxa, *Laphamia ciliata* Dewey, *L. quinqueflora* Steyermark, and *L. vitreomontana* (Warnock) I.H. Lichter-Marck were excluded from this study due to low sequence yield. As outgroup taxa, we included publicly available sequence data from GenBank sequence read archive (SRA) for *Helianthus annuus* L. of tribe Heliantheae and *Conoclinium coelestinum* DC. and *Eutrochium fistulosum* (Barratt) E.E. Lamont of tribe Eupatorieae. We extracted DNA from silica dried or herbarium leaf tissue using the DNeasy Plant Mini Kit (Qiagen, Valencia, CA, USA) or a modified version of Doyle and Doyle's (1) CTAB protocol identical to the one used by Lichter-Marck et al. (2). We prepped libraries using the HyperPrep protocol (Kapa Biosystems Inc., Wilmington, MA) in quarter reactions. Libraries were pooled 8 per reaction and enriched for 1060 low-copy nuclear genes using the COS kit (3-5) according to the directions provided by myBaits (Arbor Biosciences, Ann Arbor, MI). Enriched libraries were sent to Genewiz (South Plainfield, NJ) for massively parallel paired-end 150 bp sequencing on a HiSeq 4000, yielding >91,000 MB of raw sequencing data. Raw sequencing yields were deposited in the GenBank SRA under bioproject PRJNA918694. See Table S1 for voucher and sample SRA information.

Maximum likelihood (ML) and Bayesian inference (BI) trees were generated in RAxML-NG (6) and ExaBayes (7) using a partitioned data matrix, with each locus independently assigned a GTR+Gamma+I model of molecular evolution. The best ML tree was selected after 1000 independent searches and 1000 bootstrap replicates. The BI analysis used two independent chains to sample the posterior distribution of trees over 100,000 generations before computing a maximum clade credibility (MCC) tree based on a 50% majority rule. Gene trees used in the ASTRAL analysis were inferred separately using RAxML-NG with a GTR+Gamma+I substitution model and nodes with less than 20% bootstrap support collapsed (8). Our MCMCtree analysis used a HKY model of molecular substitution with four gamma distributed rate categories and a relaxed molecular clock conditioned on a log normally distributed rate prior (9-10). Posterior estimates of molecular substitution rates and divergence times were estimated during 200,000 generations of MCMC, and results inspected for stationarity in the program Tracer (11). To overcome computational limitations with genome scale data we subset 15 loci for use in our MCMCtree analysis using principal component axis 2 in the results of an analysis using gensortR (see ref. 12 for details).

Evolution of life history and edaphic endemism

All analyses were implemented in RevBayes (12) using the post burn-in MCC chronogram output of our MCMCtree analysis with outgroup taxa removed. Maximum a posteriori (MAP) estimates of ancestral states for both life history and edaphic endemism were based on a post burn-in posterior of 13,500 trees. We used reversible jump MCMC (rjMCMC) to assess statistical support for non-zero transition rates by alternatively setting each transition rate to zero or inferring non-zero transition rates under an exponentially distributed prior. Based on past sensitivity analyses (2), non-zero transition rates were drawn from an exponential distribution with a mean of 1 transition over the tree. Non-zero or zero rate models were inferred with equal prior probability and posterior model estimates recorded using a custom binary logical monitor. We calculated Bayes Factors as two times the natural log of the number of iterations in which a non-zero model was inferred divided by the total number of iterations (the posterior odds of model 0) divided by the number of iterations where a reversible model was inferred divided by the total number of iterations (the posterior odds of model 1), while disregarding the prior odds since we used a uniform prior. Given proven sensitivity of tests to prior information from root states (14), we based root state frequencies on ancestral state reconstructions of habitat and life-history derived from a previous study of helenioid Heliantheae (15), which showed strong prior support for tropical and

perennial states at the root of Perityleae. Transition rates under all combinations of irreversible and reversible models were inferred during 15,000 iterations of an MCMC and inspected for convergence. To improve mixing, in the presence of support for non-zero transition rates, the analysis was rerun under the non-zero transition rate prior and (MAP) ancestral states compiled from a post burn-in posterior of 13,500 trees.

To test for associations between life history and endemism on rocky outcrops we used BayesTraits (16) to compare the fit (log-likelihood) of two continuous time Markov models of life history and edaphic evolution, a dependent and independent model (17). Both models aimed to infer transitions to or from the suffrutescent perennial life-history and bare rock edaphic affinity at any given moment over infinitesimally small units of time, but the dependent model included an additional four transition-rate parameters (eight total) because it assumes that the rate of change in one trait is dependent on the state of the other. Double transitions in both traits at the same time were disallowed in both models. Given the size of the data and complexity of the models, we used reversible jump MCMC (rjMCMC) to integrate parameter estimates over the model space, weighted by their probability. Models were compared using log Bayes Factors with the equation: Log BF = 2(log likelihood dependent model – log likelihood independent model) and a log BF greater than 10 was interpreted as strong support for a correlation. For each model rjMCMC was conditioned on an exponential distribution with a mean of 100 and a hyperprior of zero. Marginal log-likelihoods were calculated using a steppingstone sampler (18) with 100 stones successively heated for 10,000 iterations.

Historical biogeography with paleo-biome informed models

Discrete biogeographical ranges for each taxon were obtained from the Southwestern Environmental Information Network (SEInet) and from an extensive review of herbarium specimens as part of the first author's systematic research on Perityleae. We scored each tip for presence in four geographical regions: South America, Baja California, the Trans-Mexican Volcanic Belt, and the Basin and Range Province (Fig. 2, S4). In South America, Perityleae has a disjunct distribution, occurring in the Atacama Desert in southern Peru and northern Chile as well as the Desventuradas Islands, ~200 km off the coast of central Chile. Baja California was defined as including the entire peninsula and nearby islands, including Guadalupe Island, the Channel Islands of southwest California, and the Revillagigedo Archipelago, located 100 km south of San Jose del Cabo. The Trans-Mexican Volcanic Belt (19) described the area covered by the predominantly volcanic mountain ranges and plateaus of northwest and central Mexico, including the Sierra Madre Occidental. The Basin and Range Province covers a wide geographic area of western North America that is characterized by its distinctive topography, with thousands of discontinuous mountain ranges punctuated by low, arid valleys (19). The Basin and Range Province here included the Madrean sky island archipelago and surrounding Sonoran Desert, the eastern continental Chihuahuan Desert and sky islands of Texas and New Mexico in the United States, and Chihuahua, Coahuila, and Tamaulipas in Mexico, as well as the numerous north-south oriented mountain ranges of the Great Basin region in Nevada and Utah, which have been called "caterpillars marching toward Mexico." (20)

Our characterization of biomes was based on the level I eco-regions of North America published by the Intergovernmental Commission for Environmental Cooperation. Desert includes the Great Basin, Sonoran, and Chihuahuan subregions, which cover broad swaths of the arid southwest United States, Baja California, and northern mainland Mexico. This biome includes both hot and cold deserts with unpredictable precipitation averaging ~250 mm or less per year and arid plant communities dominated by shrubs, stem succulents, and seasonal annuals scattered in arid, mostly open landscapes without a dense canopy cover (19). The temperate biome included high elevations of the Sierra Madre Occidental in Mexico and the Mogollon Rim in Arizona, the only areas in our study region where precipitation is predictably high, yet temperatures fall seasonally below freezing, containing plant communities dominated by coniferous or deciduous trees (19). The subtropical biome includes mid-elevation parts of the arid southwest U.S. and several states in northern and central Mexico where periodic but not extreme

drought combined with infrequent freezing temperatures produces a vegetation mosaic of grassland and shrubland with patches of forest (19). The tropical biome mostly refers to tropical deciduous forests (selva tropical subcaducifolio sensu 19), habitats where freezing temperatures do not regularly occur and seasonality in rainfall is intense, and which support a dense canopy of mostly drought deciduous trees, robust multi-stemmed shrubs, and stem succulents. In our study area, tropical deciduous forests cover the western Pacific plain of the Sierra Madre Occidental as well as the southern Cape Region and Sierra la Giganta of Baja California (19, 21-22). For a majority of Perityleae, we were able to assign each taxon to only one biome. The exceptions were wide ranging taxa, which were coded as polymorphic for multiple biomes with equal probability. One species, *Perityle emoryi*, has a distribution that overlaps with the California Floristic Province, but is mostly found in desert habitats, so we assigned it to North American desert (23). *Nesothamnus incanus,* which is endemic to the environmentally heterogeneous Guadalupe Island off the coast of Baja California, Mexico is found in low, arid habitats within the island and was therefore assigned to desert (21).

Prior to running a fully parameterized biome shift model, we first estimated rates of dispersal and extirpation among geographic areas, as well as ancestral biogeographic ranges separately from biomes using a Bayesian implementation of the Dispersal Extinction Cladogenesis (DEC) model (24) in RevBayes (13). We based our analyses on the MAP chronogram output of our MCMCtree analysis. Given evidence that transitions into the null range can result in abnormal extirpation rates and range sizes, we conditioned our analysis on survival by setting the probability of entering the null range to zero (25). Our implementation of the DEC modeled anagenetic dispersal and local extinction (extirpation) rates and was based on a log-uniform prior and considered only allopatry and subset sympatry as potential cladogenetic events (see 26 for rationale). Dispersal and extirpation rates, cladogenetic events, and ancestral biogeographic ranges were inferred during 30,000 iterations of an MCMC. Estimates of ancestral ranges at nodes and shoulders were compiled from 28,000 samples of post burn-in posterior trees and the results plotted using the R package RevGadgets (27, Fig. S4).

To explicitly test the hypothesis that shifts into the desert biome tracked the availability of desert habitats through time, we performed a sensitivity analysis using rjMCMC to model two alternative scenarios: a) total dependence of biome-shifts on paleo-biome structure through time and b) total independence of shifts on paleo-biome structure through time. To model independence we used the set.value() function in RevBayes to fix parameter w_b at 0 and parameters w_u and w_g at 0.5, and to model dependence w_b was assigned a value of 1 and w_u and w_g a value of 0. We then estimated transition rates among biomes and generated model averaged ancestral states across the four geological time intervals using 25,000 generations of rjMCMC, with either model weighted with equal prior probability. We checked for convergence in the program Tracer (11) and two times the Log Bayes Factor was calculated as the posterior probability of the independent model (the number of MCMC samples that visited the independent model divided by the total number of samples) divided by the posterior probability of the dependent model (calculated likewise). Equal prior probability was placed on the two models, therefore the prior ratio was not included in the computation of the BF. Following Kass and Raftery (51), 2logBFs were interpreted as: zero to two, equivocal for a non-zero transition rate; two to six, strong support for non-zero transition rate; greater than six, decisive support for a non-zero transition rate.

Supplemental results and discussion

Taxonomic implications of a more densely sampled phylogeny of Perityleae

Resolution of a diverse early diverging lineage that tracked the separation of the Baja California peninsula reinforces the recently improved understanding of Perityleae that required revision of taxonomic concepts (28). Until recently, most of the species diversity in Perityleae was recognized within the “core” genus *Perityle,* but non-monophyly of *Perityle* and support for the type species, *Perityle californica*, as nested within an early diverging Baja California clade was

the basis for several changes, including: a narrowed circumscription of *Perityle,* recognition of the long-branch *Nesothamnus,* and reinstatement of *Galinsogeopsis* and *Laphamia* with new, broader delimitations. Expanded sampling of the Baja California clade using target capture in the current study also supports the inclusion within *Perityle* of *P. socorrensis* Rose*, P. emoryi* Torr.*, Perityle tenuifolius* (Phil.) Lichter-Marck, and the three taxa of genus *Amauria* Benth. (22, 28). *Perityle* remains non-monophyletic as currently circumscribed, with *Perityle rosei* Greenm. and *P. trichodonta* S.F. Blake resolved as more closely related to *Pericome* and *Eutetras* than to other members of *Perityle.* The monotypic, Guadalupe Island endemic *Nesothamnus incanus* (A. Gray) Rydb. occupies a long branch that is the sister lineage to *Galinsogeopsis*.

Non-monophyly of densely sampled taxa

Inclusion of multiple conspecific samples in the present study showed support for monophyly of recognized species in most cases, but there were several species for which samples did not group together. Taxa found to be non-monophyletic include *Galinsogeopsis feddemae* (McVaugh) I.H. Lichter-Marck, *Laphamia cordifolia* (S.F. Blake) I.H. Lichter-Marck, *L. gracilis* M.E. Jones, *L. lemmonii* A. Gray, *L. megalocephala* S. Watson, *L. rupestris* A. Gray, *Perityle cuneata*, *P. emoryi, and P. rosei*. In part, these results reflect our choice to sequence samples representative of morphologically unique and geographically disjunct populations collected during the first author's field work and examination of herbarium collections. Perityleae tend to grow in unreachable parts of the most inaccessible cliffs and canyons in the North American deserts, where their isolated populations are arrayed across 2000 miles of dry and mostly roadless terrain punctuated by imposing rocky mountains (28). Comprehensive floristic studies of sky islands and parts of the Sierra Madre Occidental have led to the description of many new-to-science species of Perityleae since the tribe was last treated by Powell (e.g., 29), and our results suggest that the currently recognized diversity of Perityleae continues to be underestimated. Our fragmentary knowledge of the diversity in this group is a conservation concern because Perityleae habitats are imminently threatened by energy development, climate change, and mining. With >30% of the species in this group listed as vulnerable, imperiled, or critically endangered on NatureServe, Perityleae stands out as having one of the highest proportions of at-risk taxa of any taxon in the arid western North American flora.

Widespread occurrence of edaphic specialization on bare habitats among close relatives to predominantly desert plant and animal lineages

Familiar desert plant lineages are dominant elements in the flora of rocky outcrops in the tropical deciduous forests that are adjacent to, and considered a major source area for expansions into, the North American deserts (30), including cacti (Cactaceae; e.g. *Echinocereus bacanorensis* (W. Rischer & Trocha) W. Blum and *Mammillaria grahamii* Engelm.), agaves (Agavaceae; e.g. *Agave aurea* Brandegee), euphorbias (Euphorbiaceae; e.g. *Euphorbia chaetocalyx* var. *triligulata* (L.C. Wheeler). M.C. Johnst.), legumes (Leguminosae; e.g. *Erythrina flabelliformis* Kearney), cheilanthoid ferns (Pteridaceae; e.g. *Astrolepis sinuata* Sw., *Notholaena aurantiaca* D.C. Eaton, *Myriopteris myriophylla* (Desv.) J.Sm., and *Argyrochosma peninsularis* (Maxon & Weath.) Windham), composites (Compositae; e.g. *Brickellia brandegeei* B.L. Rob., *Coreocarpus dissectus* S.F. Blake, and *Xanthisma incisifolium* (I.M. Johnst.) G. Nesom), evening primroses (Onagraceae; e.g. *Oenothera toumeyi* Tidestr. and *Gongylocarpus fruticulosus* Brandegee), mints (Lamiaceae; *Hedeoma drummundii* Benth.), stonecrops (Crassulaceae; e.g. *Graptopetalum rusbyi* Rose, *Echeverria colorata* E. Walther*,* and *Dudleya nubigena* Britton & Rose), chuparosas (Acanthaceae; e.g. *Justicia sonorae* Wassh.), turpentine-brooms (Rutaceae; e.g. *Thamnosma ciliata* I.M. Johnst.), and datillos (Bromeliaceae; e.g., *Hechtia* jaliscana L. B. Sm.). Decomposed, but typically open edaphic substrates such as gypsum, greenstone, and limestone outcrops, alkaline sinks, and volcanic talus also harbor members or close relatives of predominantly desert plant lineages in adjacent more densely vegetated biomes, including *Tiquilia* (Ehretiaceae; e.g. *T. gossypina* clade), *Encelia* (Compositae; e.g. *Enceliopsis* spp.), ivesioids (Rosaceae; *Potentilla* spp.), jewelflowers (Brassicaceae; Thelypodieae), *Nama* (Namaceae; e.g. *Nama rupicola* Bonpl. ex Choisy), and *Zeltnera* (Gentianaceae; e.g. *Zeltnera*

calycosa (Buckley) G. Mans.). Similar patterns can be found in groups of predominantly desert animals, such as rattlesnakes, lizards, geckos, and tortoises, which are often found closely associated with rocky outcrops in a tropical context, though arboreal lifestyles may have also played a role in pre-adapting these lineages for success in the desert ecosystem (31). Putative adaptations for growth on bare rock include stress tolerant leaf traits, such as dense hairs, small waxy leaves, or lack of leaves, a caespitose growth form, shifts towards self-compatibility, and heightened anti-herbivore defenses (see ref. 32 for a recent review). In groups that show edaphic specialization for bare or chemically harsh edaphic outcrops, such innovations in stress tolerance may provide the mechanism for shifts into new, taxing environments where there is less competition or additional pressures that facilitate innovation, and therefore create opportunity for rapid radiation (32).

Fig. S1. Additional photographs illustrating habit and habitat diversity within the predominantly desert and tropical deciduous forest dwelling rock daisy genus *Laphamia*. (A) A scattered rocky outcrop within otherwise densely vegetated tropical deciduous forest in the Sierra de Alamos, Sonora, Mexico. (B) Growth out of the exposed cliffs on the eastern side of the outcrop shown in (A) of *Laphamia cordifolia*. (C) An herbarium specimen showing the perennating woody caudex of suffrutescent perennial Perityleae that is associated with growth on bare, rocky outcrops. (D) A rock outcrop plant community in a tropical deciduous forest in Sonora, Mexico including members

of the following otherwise predominantly desert plant groups: cacti (Cactaceae, *Echinocereus bacanorensis*), cheilanthoid ferns (Cheilanthoideae, *Myriopteris lindheimeri),* and rock daisies (Perityleae, *Laphamia reinana*). (E) *Laphamia gentryi* growing on a rocky outcrop surrounded by (F) tropical deciduous forest in the western Sierra Madre Occidental in Sonora, Mexico. (G) Cliffs and cathedrals of rhyolite in the Chiricahua Mountains in Arizona, U.S.A. (H) *Laphamia cochisensis,* a narrow endemic to the Chiricahua Mountains growing out of bare, rhyolitic cliffs. (I) View of surrounding subtropical forest from the vantage point of *Laphamia cochisensis.* (J) Limestone outcrops of the Great Basin Desert in the Inyo Mountains, California, U.S.A. (K) *Laphamia intricata* (left foreground) growing on calcareous outcrops in the Ivanpah Mountains, California, U.S.A. (L) *Laphamia villosa*, a narrow endemic found only on limestone outcrops in the Panamint Range, California, U.S.A.

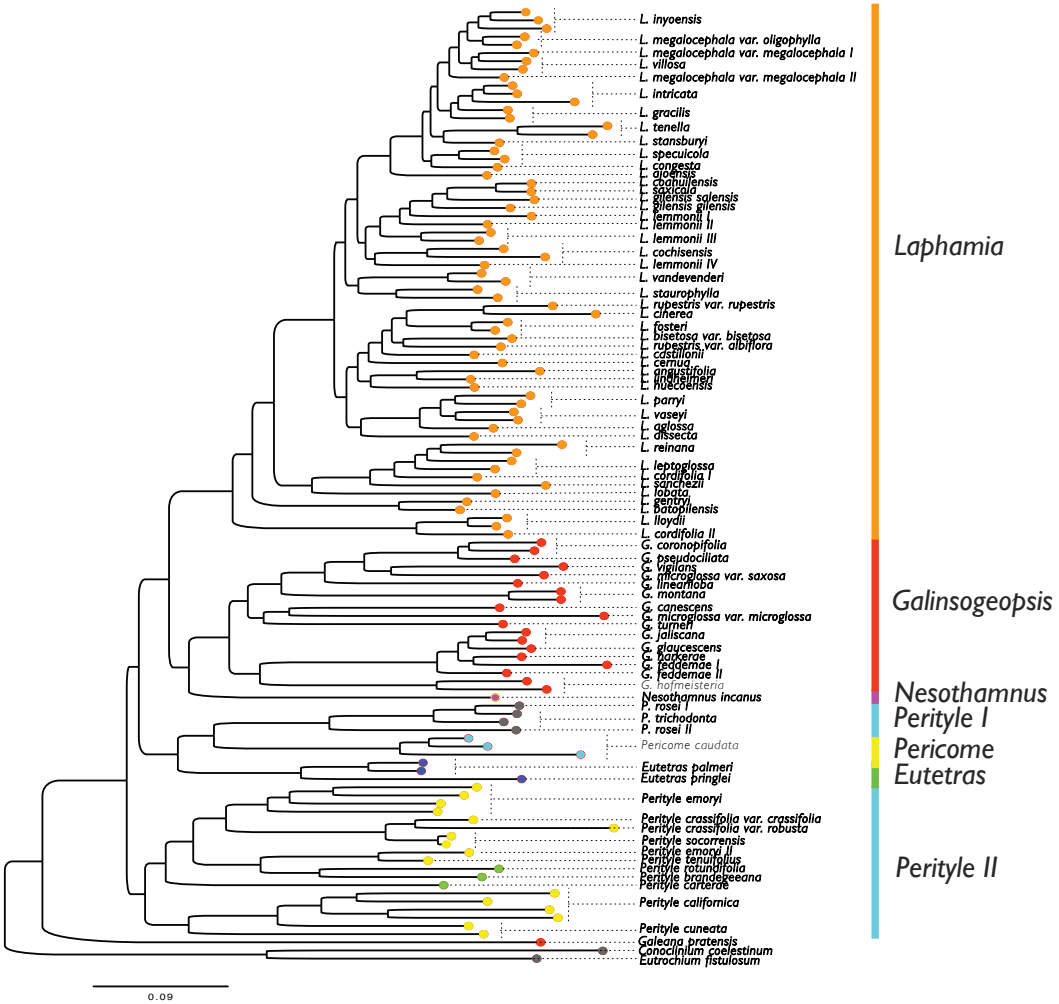

Fig. S2. Phylogeny of Perityleae based on concatenated analysis of 229 low-copy nuclear supercontigs combining both exons and introns using Bayesian statistical inference in the program ExaBayes (7). The data matrix on which this analysis was based was ~1,400,000 bp. Posterior probabilities were estimated during 1,000,000 iterations of MCMC and checked for stationarity in the program Tracer (11). Posterior probabilities of 1 were recovered at all nodes. Color coded tips denote genera in the recent classification by Lichter-Marck (28).

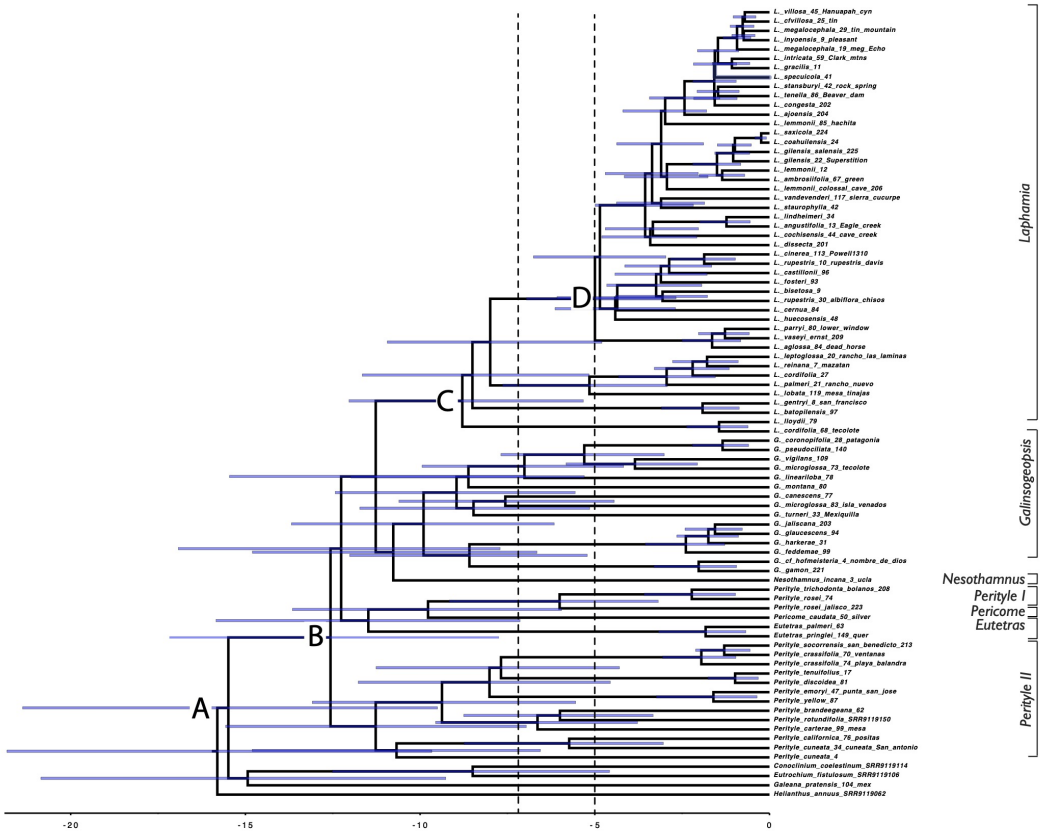

Fig. S3. Time calibrated phylogeny of Perityleae based on a fixed topology derived from a pseudocoalescent analysis of 229 low-copy nuclear genes inferred with Astral-III (8). Divergence times were estimated using the software program MCMCtree and based on a subset of 15 loci selected using multivariate phylogenetic subsampling with the program genesortR in the R statistical environment (R Core Team 2019))(9-10,12; Table S2). Our analysis was conditioned on an uncorrelated log normal relaxed molecular clock and an HKY molecular substitution model with four gamma distributed rate categories. A secondary node calibration of 7.93–23.22 Ma (95% HPD) derived from recent analyses of the Heliantheae alliance by Landis et al. (33) was applied to the split of *Helianthus annuus* from Eupatorieae + Perityleae. Posterior estimates of divergence times were obtained during 45,000 iterations of post-burnin MCMC and the analysis repeated to check for comparable results. Dotted lines indicate the timing of onset of widespread arid conditions in western North America. Annotations accompany nodes mentioned in the text: (A) the root node corresponding to the most recent common ancestor of tribes Perityleae+Eupatorieae and *Helianthus annuus* L. (B) The split between the two major lineages of rock daisies in genus *Perityle* from the clade containing *Laphamia, Galinsogeopsis, Nesothamnus, Eutetras*, and *Pericome*. (C) The crown age of genus *Laphamia*. (D) The most recent common ancestor of desert rock daisies in the genus *Laphamia*.

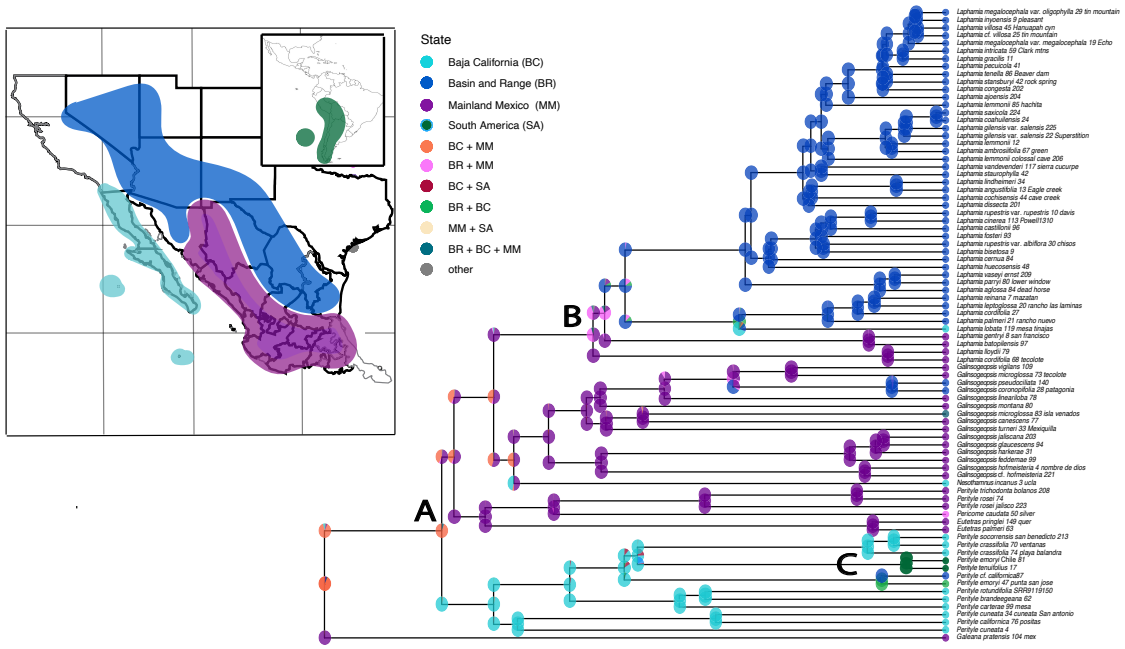

Fig. S4. Ancestral state reconstruction of biogeographic ranges of rock daisies at nodes and shoulders based on 28,000 post-burnin MCMC iterations of a dispersal-extinction-cladogenesis model implemented in RevBayes. A range map indicates the extent of the four regions included in the analysis: Baja California Peninsula (light blue), the Basin and Range Province (dark blue), mainland Mexico (purple), and South America (dark green). Pie graphs show ranges proportional to their posterior probability, with cladogenetic events indicated as instances where the daughter ranges at shoulders differ from the common ancestor's range at their intervening node. Our analysis was based on the MAP chronogram output of our MCMCtree analysis, with a probability of entering the null range set to zero (25), and anagenetic dispersal and local extinction (extirpation) inferred with a log-uniform prior. Only allopatry and subset sympatry were considered as potential cladogenetic events in this analysis (see 26 for rationale). Annotated nodes correspond to those mentioned in the text: (A) a cladogenetic (subset sympatry) event resolved at this node separates the principal radiations of rock daisies, which have distributions centered on mainland Mexico and Baja California. (B) Dispersal of *Laphamia* into the Basin and Range Province out of mainland (northwestern) Mexico. (C) Long distance dispersal of rock daisies from North America to South America.

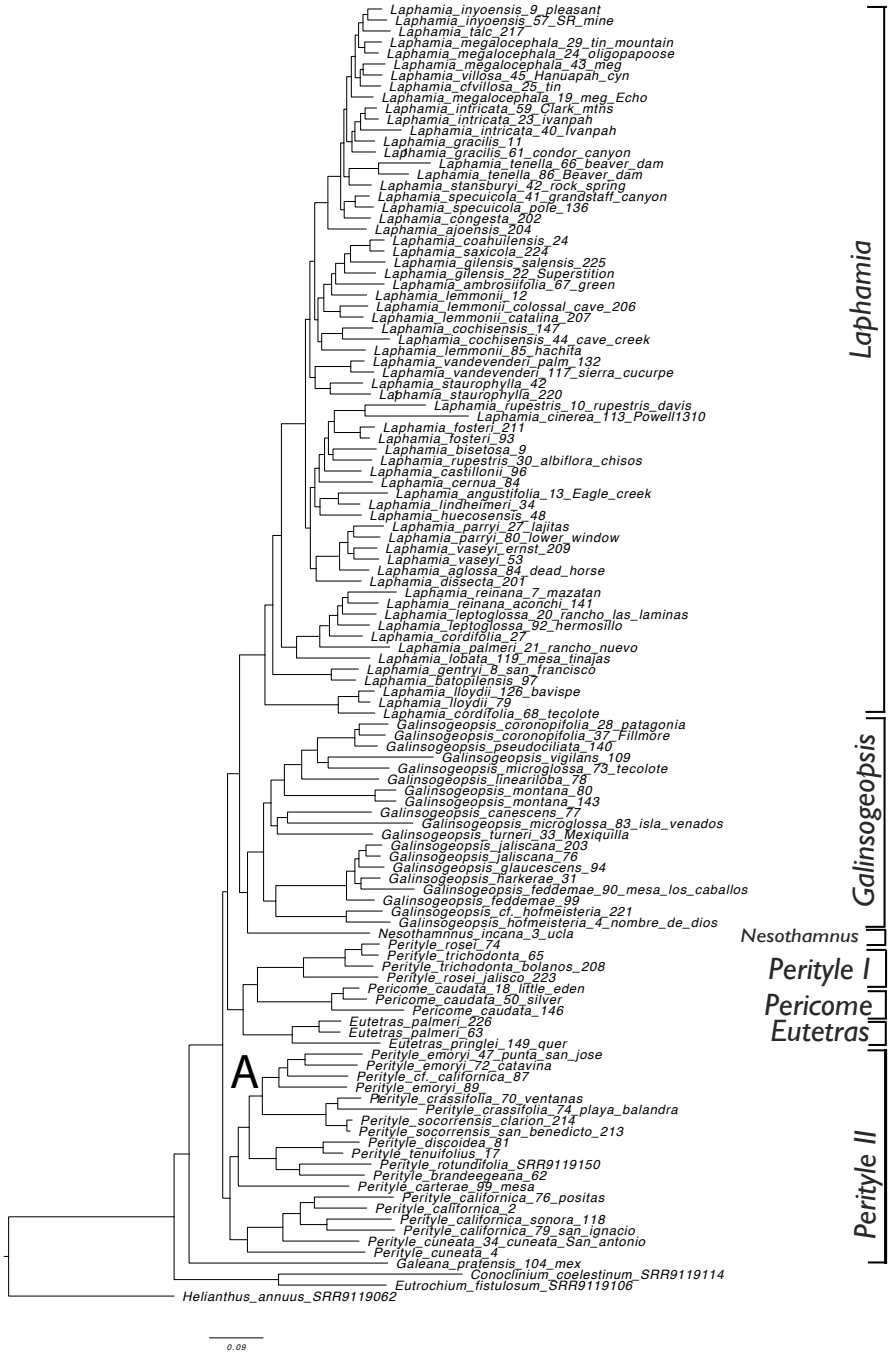

Fig. S5. Maximum clade credibility phylogeny of Perityleae based on a partitioned data matrix of 229 low-copy nuclear loci inferred from 1,000,000 generations of MCMC in ExaBayes (7). Posterior probabilities equal to one were inferred at all nodes. The analysis used two independent chains to sample the posterior distribution before computing a maximum clade credibility tree based on a 50% majority rule. (A) Position of the widespread allopolyploid *Perityle emoryi*, a major topological incongruence with the pseudocoalescent (ASTRAL) analysis, which resolves *P. emoryi* and the sample tentatively determined as *P.* cf. *californica* as the sister lineage to *Laphamia*.

Fig. S6. Maximum likelihood phylogeny of Perityleae inferred using RAxML-NG based on a partitioned data matrix of 229 low-copy nuclear genes with each locus independently assigned a GTR+gamma+I molecular substitution model. The best ML tree was selected after 1000 independent searches and 1000 bootstrap replicates. Nodes with bootstrap support less than 90 are annotated with their corresponding support values. (A) Position of the widespread allopolyploid *Perityle emoryi*, a major topological incongruence with the pseudocoalescent (ASTRAL) analysis, which resolves *P. emoryi* and the sample tentatively determined as *P.* cf. *californica* as the sister lineage to *Laphamia*.

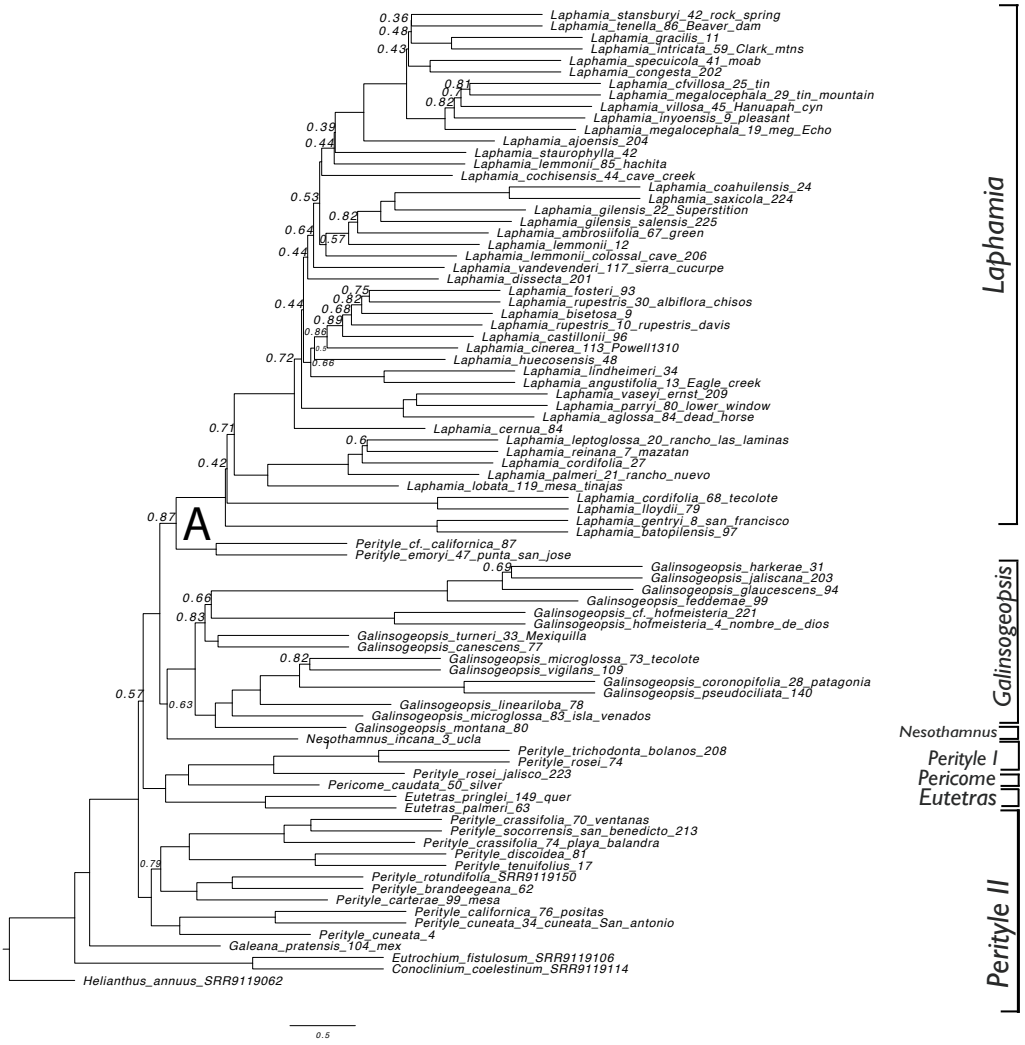

Fig. S7. Pseudo-coalescent phylogeny of Perityleae based on ASTRAL-III analysis of 229 gene trees inferred separately in RAxML under a GTRCAT substitution model. Nodes in gene trees with less than 20% bootstrap support were collapsed (8). Values at nodes reflect concordance factors and are shown for cases where proportional concordance was less than 0.9. (A) Position of the widespread allopolyploid *Perityle emoryi* and a sample tentatively identified as *P.* cf. *californica,* a major topological incongruence with concatenated analyses, which resolve both samples as nested within *Perityle*.

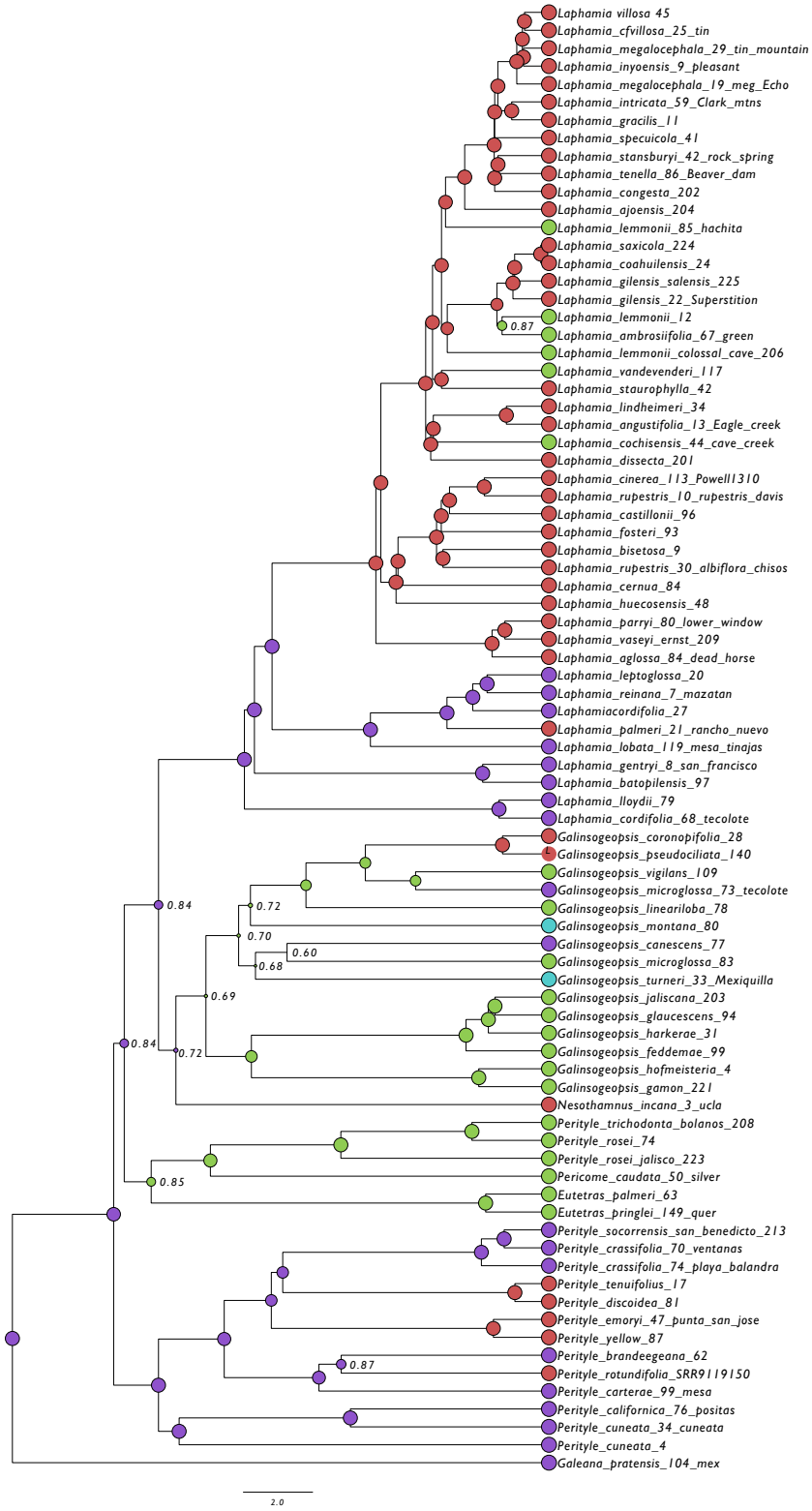

Fig. S8. Maximum a posteriori reconstruction of ancestral habitat in Perityleae estimated from 13,500 post-burnin iterations of reversible jump MCMC in RevBayes. Purple = tropical, green = subtropical, blue = temperate, and red = desert. Sizes of circles indicate posterior probabilities with values at nodes indicated when proportional support was less than 0.9.

Table S1. Voucher information, and GenBank SRA accession numbers for sampled individuals of Perityleae sequenced for this study. See ref. 2 for information on samples included from this previous study. Herbarium acronyms follow Thiers, B. [continuously updated]. Index Herbariorum: A global directory of public herbaria and associated staff. New York Botanical Garden's Virtual Herbarium. http://sweetgum.nybg.org/science/ih/

Taxon	Accession or collection #	Location	Herbarium	Collector(s)	Collection date	GenBank SRA Accession # (PRJNA918694)
Eutetras palmeri A. Gray	UCR 117599	Rincón de Ramos, Aguascalientes, MX	UCR	J.L. Villaseñor R.	22 October 1995	SAMN32604225
Eutetras palmeri A. Gray	UCR 117599	Aguascalientes, MX	UCR	J.L. Villaseñor R.	October 22 1995	SAMN32604226
Galinsogeopsis canescens (Everly) I.H. Lichter-Marck	UC 651747	Sierra Tacuichamona, Sinaloa, MX	UC	H.S. Gentry	12 February 1940	SAMN32604211
Galinsogeopsis coronopifolia (A.Gray) I.H. Lichter-Marck	ILM 394	Organ Mountains, Doña Ana Co., NM, USA	UC	I.H. Lichter-Marck & I. Nunez	October 2018	SAMN32604206
Galinsogeopsis feddemae (McVaugh) I.H. Lichter-Marck	NY 426075	Valparaiso, Zacatecas, MX	NY	C. Feddema	16 August 1969	SAMN32604216
Galinsogeopsis glaucescens (B.H. Turner) I.H. Lichter-Marck	TEX 29908	Juchipilas, Zacatecas, MX	TEX	J. Panero	7 November 1996	SAMN32604215
Galinsogeopsis jaliscana (A. Gray) I.H. Lichter-Marck	ILM 603	Sierra de San Esteban, Jalisco, MX	UC	I.H. Lichter-Marck, P. Carrilo-Reyes, K. Soler, S. Winitsky	November 2018	SAMN32604213
Galinsogeopsis jaliscana (A. Gray) I.H. Lichter-Marck	Lundell 60080	El Diente de Sierra de San Esteban, Jalisco, MX	Lundell	A. García G., M. Dolores A.	8 February 1994	SAMN32604214
Galinsogeopsis lineariloba (Rydb.) I.H. Lichter-Marck	UC145620	San Ramon, Durango, MX	UC	E. Palmer	21 April-18 May 1906	SAMN32604208
Galinsogeopsis montana (A.M. Powell) I.H. Lichter-Marck	UC 1523222	Turuachi, Chihuahua, MX	UC	G. Nesom & P. Lewis	24 Aug 1984	SAMN32604209
Galinsogeopsis montana (A.M.	TEX 00141967	Turuachi Canyon, Chihuahua, MX	TEX	G. Nesom & P. Lewis	24 August 1984	SAMN32604210

Powell) I.H. Lichter-Marck						
Galinsogeopsis pseudociliata (A.M. Powell) I.H. Lichter-Marck	ARIZ356412	Sierra La Brena on E slope of the Sierra Madre, Chihuahua, MX	AZ	J. Spencer; D. Atwood	25 September 1998	SAMN32604207
Galinsogeopsis sp. nov. "gamon"		Sierra de Gamon, Durango, MX	CIIDIR	A. Castro-Castro		SAMN32604217
Galinsogeopsis spilanthoides var. *spilanthoides* Sch. Bip.	CIAD 2652	Isla Venados, Mazatlan, Sinaloa, MX	CIAD	M. Ruiz Guerrero.	5 February 2017	SAMN32604212
Laphamia ajoensis (Todsen) I.H Lichter-Marck	ILM	Ajo Mountains, Pima Co., AZ, USA	UC	I.H Lichter-Marck & S. Winitsky	December 2020	SAMN32604178
Laphamia bisetosa A. Gray	UC 1412751	Maravillas Canyon, Brewster Co., TX, USA	UC	D.S. Correll & H.B. Correll	9 November 1967	SAMN32604194
Laphamia cernua Greene	ILM 393	Organ Mountains, Doña Ana Co., NM, USA	UC	I.H. Lichter-Marck	September 2019	SAMN32604195
Laphamia cf. *inyoensis* Ferris	ILM 105	Talc City, Inyo Co., CA, USA	UC	I.H. Lichter-Marck & K. Allerton	July 2018	SAMN32604168
Laphamia coahuilensus (A.M. Powell) I.H. Lichter-Marck	AZ 337203	Sierra de San Marcos, Coahuila, MX	AZ	M.C. Johnston, T. Wendt, & F. Chiang.	12 June 1972	SAMN32604179
Laphamia cochisensis W.E. Niles	ILM 789	Chiricahua Mountains, Cochise Co., AZ, USA	UC	I.H. Lichter-Marck & J. Santore	August 2019	SAMN32604186
Laphamia congesta M.E. Jones	ILM 874	South Rim, Grand Canyon, Coconino Co., Arizona, USA	UC	I.H Lichter-Marck & S. Winitsky	September 2019	SAMN32604177
Laphamia cordifolia (Rydb.) I.H. Lichter-Marck	AZ 347845	Yecora, Sonora, MX	AZ	A.L. Reina-G.; T.R. Van Devender, T.F. Daniel, G.M. Ferguson, B.J. Syke	17 March 1998	SAMN32604204
Laphamia cordifolia	UCR 80496	Sierra de Alamos, Sonora, MX	UCR	A.C. Sanders	20 March 1993	SAMN32604205

(Rydb.) I.H. Lichter-Marck						
Laphamia dissecta Torr.	Black s.n.	Lajitas, Presidio Co., TX, USA	SRSU	A. Black	11 August 2019	SAMN32604201
Laphamia fosteri (A.M. Powell) I.H. Lichter-Marck	TEX 6528	Panther Canyon, Apache Mountains, Culberson Co., TX, USA	TEX	J.F. Weedin	1978	SAMN32604192
Laphamia fosteri (A.M. Powell) I.H. Lichter-Marck	SRSU 1233	Panther Canyon, Apache Mountains, Culberson Co., TX, USA	SRSU	A.M. Powell	1978	SAMN32604193
Laphamia gilensis var. *gilensis* (M.E. Jones)	UCR 138793	Tortilla Flat, Superstition Mountains, AZ, USA	UC	W. Hodgson	15 April 1993	SAMN32604182
Laphamia gilensis var. *salensis* (A.M. Powell) I.H. Lichter-Marck	ILM 314	Salt River, Apache Co., AZ, USA	UC	I.H. Lichter-Marck	August 2018	SAMN32604181
Laphamia gracilis M.E. Jones	UC 1582885	Sheep Range, Clark Co., NV, USA	UC	T.L. Ackerman	2 July 1979	SAMN32604174
Laphamia huecosensis (A.M. Powell) I.H. Lichter-Marck	UC 1609992	Sierra Juarez, Chihuahua, MX	UC	R. Spellenberg, L. Brouillet, D. Kearns.	29 May 1993	SAMN32604197
Laphamia intricata Brandegee	ILM 229	Ivanpah Mountains, San Bernardino Co., CA, USA	UC	I.H. Lichter-Marck	August 2018	SAMN32604172
Laphamia intricata Brandegee	ILM 230	Ivanpah Mountains, San Bernardino Co., CA, USA	UC	I.H. Lichter-Marck	August 2018	SAMN32604173
Laphamia inyoensis Ferris	ILM 48	Pleasant Mountain, Inyo Co. CA, USA	UC	I.H. Lichter-Marck & K. Allerton	July 2018	SAMN32604167
Laphamia lemmonii A. Gray	UC 709590	Graham Mountains, Graham Co., AZ, USA	UC	R.M. McGuire.	2 June 1935	SAMN32604183
Laphamia lemmonii A. Gray	ILM 310	Colossal Cave, Pima Co., AZ, USA	UC	I.H. Lichter-Marck	August 2018	SAMN32604184
Laphamia lemmonii A. Gray	ILM 274	Catalina Mountains, Pima Co., AZ, USA	UC	I.H. Lichter-Marck & S. Winitsky	December 2020	SAMN32604185

Laphamia lemmonii A. Gray	ILM 458	Big Hatchet Mountains, Hidalgo Co., NM, USA	UC	I.H. Lichter-Marck	August 2018	SAMN32604187
Laphamia leptoglossa (Harv. & A. Gray ex A. Gray) I.H. Lichter-Marck	MDE-2708	Sierra la Campana, Hermosillo, Sonora, MX	SON	T.R. Vandevender	25 December 2015	SAMN32604203
Laphamia lindheimeri A. Gray	UC 1440574	Loma Alta, Val Verde Co., TX, USA	UC	A.M. Powell & S. Sikes	19 June 1965	SAMN32604196
Laphamia megalocephala var. *megalocephala* S. Watson	ILM 334	Echo Canyon Reservoir, Pioche, NV, USA	UC	I.H. Lichter-Marck	September 2018	SAMN32604171
Laphamia megalocephala var. *oligophylla* (A.M. Powell) I.H. Lichter-Marck	ILM 204	Tin Mountain, Inyo Co., CA, USA	UC	I.H. Lichter-Marck & K. Allerton	July 2018	SAMN32604169
Laphamia megalocephala var. *oligophylla* (A.M. Powell) I.H. Lichter-Marck	ILM 166	Papoose Flat, Inyo Co., CA, USA	UC	I.H. Lichter-Marck & K. Allerton	July 2018	SAMN32604170
Laphamia palmeri A. Gray	ILM 339	Beaver Dam Mountains, Washington Co., UT, USA	UC	I.H. Lichter-Marck	September 2018	SAMN32604175
Laphamia parryi (A. Gray) Benth. & Hook.	ILM 377	Chisos Mountains, Brewster Co., TX, USA	UC	I.H. Lichter-Marck & S. Winitsky	October 2018	SAMN32604198
Laphamia reinana (B.L. Turner) I.H. Lichter-Marck	Santore s.n.	Sierra los Locos, Mncpio. Aconchi, Sonora, MX	UC	J. Santore	August 2019	SAMN32604202
Laphamia rupestris var. *rupestris* A. Gray	AZ 283476	Davis Mountains, Davis Co., TX, USA	AZ	S. Sikes	September 1965	SAMN32604191
Laphamia saxicola Eastw.	AZ 372727	Superstition Mountains, Maricopa Co., AZ, USA	AZ	M. Quinn	17 April 2003	SAMN32604180
Laphamia specuicola (S.L. Welsh &	ILM 322	Moab, Grand Co., UT, USA	UC	I.H. Lichter-Marck	September 2018	SAMN32604176

Neese) I.H. Lichter-Marck						
Laphamia staurophylla Barneby	ILM 802	Truth or Consequences, NM., USA	UC	I.H. Lichter-Marck	September 2019	SAMN32604189
Laphamia staurophylla Barneby	UC 1731838	Fresnal Canyon, Alamagordo, Otero Co., NM, USA	UC	Dean Wm. Taylor	21 July 1991	SAMN32604190
Laphamia vandevenderi (B.H. Turner) I.H. Lichter-Marck	Vandevender 2018- 87	Sierra Cucurpe, Sonora, MX	US	T. Vandevender & A.L. Reina	August 2017	SAMN32604188
Laphamia vaseyi (J.M. Coult.) I.H. Lichter-Marck	AZ 416297	Plateau south of Cigar Mountain, Brewster Co., TX, USA	AZ	Mark Fishbein; Angela Rein, Lindsey Worcester	14 August 2013	SAMN32604199
Laphamia vaseyi (J.M. Coult.) I.H. Lichter-Marck	ILM 355	Ernst Tinaja, Brewster Co., TX, USA	UC	I.H. Lichter-Marck & S. Winitsky	October 2018	SAMN32604200
Nesothamnus incanus (A. Gray) Rydb.	ILM	UCLA Botanical Garden, Los Angeles, CA, USA	UC	I.H. Lichter-Marck & E. Meyer	May 2019	SAMN32604218
Pericome caudata B.L. Rob.	ILM 118	Silver Canyon, White Mountains, Inyo Co., CA, USA	UC	I.H. Lichter-Marck, K. Allerton, D. Neubauer	July 2018	SAMN32604223
Pericome caudata B.L. Rob.	ILM 769	Little Eden Spring, Humphrey's Peak, Coconino Co., AZ, USA	UC	I.H. Lichter-Marck	September 2018	SAMN32604224
Perityle brandegeeana Rose	UCR 146783	Baja California Sur, MX	UCR	N/A		SAMN32604235
Perityle californica Benth.	Reina 2019-04	Cerro Colorado, Sonora, MX	US	A.L. Reina & T. Vandevender	Jan 2019	SAMN32604236
Perityle californica Benth.	ILM 692	San Ignacio, Baja California, MX	UC	I.H. Lichter-Marck	Jan 2019	SAMN32604237
Perityle californica Benth.	UC 1787616	Ciudad Constitucion, Baja California Sur, MX	UC	J.P. Rebman	24 October 2001	SAMN32604238
Perityle cf. californica Torr.	JEPS 128783	Chocolate Mountains, Imperial Co., CA, USA	UC	A. Sanders, J. Malusa, & I.H. Lichter-Marck	March 2017	SAMN32604230

Perityle cuneata var. *marginata* (Rydb.) I.M. Johnst.	UC 1116153	Playa el Coyote, La Paz, Baja California Sur, MX	UC	D.M. Porter	30 December 1958	SAMN32604239
Perityle emoryi Torr.	UC 648836	Caldera, Atacama Province, Chile	UC	A.A. Beetle	19 February 1939	SAMN32604227
Perityle emoryi Torr.	ILM2017-3	Punta San Jose, Baja California, MX	UC	I.H. Lichter-Marck	May 2017	SAMN32604228
Perityle emoryi Torr.	ILM 693	Cataviña, Baja California, MX	UC	I.H. Lichter-Marck	January 2019	SAMN32604229
Perityle emoryi Torr.	ILM 191	Hanuapah Canyon, Inyo Co., CA, USA	UC	I.H. Lichter-Marck & K. Allerton	June 2018	SAMN32604231
Perityle rosei Greenm.	ILM 621	Sierra la Primavera, Jalisco, MX	UC	I.H. Lichter-Marck & P. Carrillo-Reyes	November 2018	SAMN32604219
Perityle rosei Greenm.	CAS 694453	Heujuquilla del Alto, Durango, MX	CAS	D.E. Breedlove, F. Almeda	23 November 1983	SAMN32604220
Perityle socorrensis Rose	SD 259737	Isla San Benedicto, Colima, MX	SD	J. Rebman, E. Excurra, S.Vanderplank		SAMN32604232
Perityle socorrensis Rose	SD 259739	Isla Clarion, Colima, MX	SD	J. Rebman, E. Excurra, S. Vanderplank		SAMN32604233
Perityle tenuifolius (Phil.) I.H. Lichter-Marck	SD	Isla San Felix, Desventuradas Islands, Chile	SD	R. Thorne		SAMN32604234
Perityle trichodonta S.F. Blake	ILM 615	Bolaños, Jalisco, MX	UC	I.H. Lichter-Marck, P. Carrillo-Reyes, K. Soler, S. Winitsky	November 2018	SAMN32604221
Perityle trichodonta S.F. Blake	UCR 70576	Nayarit, a 22.7 km al SW de Jesus Maria, Camino a la Mesa del Nayar, MX	UCR	O. Téllez V., G. Flores F.	5 November 1988	SAMN32604222

Table S2. A summary of descriptive statistics for low-copy nuclear loci obtained by next-generation sequencing (target enrichment) with the Compositae Conserved Orthologous Set (COS) and used in full and subset data matrices to infer phylogenies of the rock daisies (3-5). Individual loci were aligned using MAFFT (34) under default settings. Characteristics of gene trees were based on phylogenies inferred separately for each locus in RAxML-NG with a GTR+Gamma+I substitution model (6). Estimation of gene properties were performed in the R statistical environment (R Core Team 2019) with the genestortR pipeline (see ref. 12 for specific details on the analyses).

Data matrix	**Summary statistic**	**Measured on**	**Mean**	**Median**	**Standard Deviation**
Full dataset (118 tips; 229 loci; 1,419,391 total bp DNA)	Average alignment length (base pairs DNA)	Alignments	5856.96	4881	+/- 3598.44
	Missing data (proportion of sites with missing or ambiguous data)	Alignments	0.72	0.73	+/-0.08
	Number of taxa	Alignments	82.68	82.93	**+/-** 1.66
	Variability (Proportion of variable sites)	Alignments	0.45	0.44	**+/-** 0.1
	Total tree length (substitutions)	Gene trees	7.48	6.56	**+/-**3.99
	Level of treeness (fraction of tree length on internal branches)	Gene trees	0.34	0.33	**+/-**0.06
	Sensitivity to long branch attraction (average pairwise patristic distance between terminals)	Gene trees	0.45	0.4	**+/-**0.26
	Clock-likeness (variance of root-to-tip distances)	Gene trees	0.05	0.03	**+/-**0.07
	Level of saturation (one minus the regression slope of patristic distances on p-distances [proportion of mismatches])	Alignments and gene trees	0.73	0.74	**+/-**0.1
	Average support (mean bootstrap value)	Gene trees	57.21	57.23	**+/-**8.72
Reduced subset (85 tips; 15 loci; 68,414 total bp DNA)	Average alignment length (base pairs DNA)	Alignments	3820.93	3451	**+/-** 1978.16
	Missing data (proportion of sites with missing or ambiguous data)	Alignments	0.69	0.70	0.08
	Number of taxa	Alignments	83.07	82.93	**+/-**1.62
	Variability (proportion of variable sites)	Alignments	0.48	0.47	**+/-**0.08

	Total tree length (substitutions)	Gene trees	5.94	5.85	**+/-**2.22
	Level of treeness (fraction of tree length on internal branches)	Gene trees	0.29	0.3	**+/-**0.04
	Sensitivity to long branch attraction (Average pairwise patristic distance between terminals)	Gene trees	0.34	0.30	**+/-**0.19
	Clock-likeness (variance of root-to-tip distances)	Gene trees	0.03	0.01	**+/-**0.05
	Level of saturation (one minus the regression slope of patristic distances on p-distances [proportion of mismatches])	Alignments and gene trees	0.65	0.65	**+/-**0.14
	Average support (mean bootstrap value)	Gene trees	41.66	40.7	+/-4.6

SI References

Sample References:

1. J.J. Doyle, J.L. Doyle, CTAB DNA extraction in plants. *Phytochemical Bulletin,* 19, 11–15 (1987).
2. I.H. Lichter-Marck, W.A. Freyman, C.M. Siniscalchi, J.R. Mandel, A. Castro-Castro, G. Johnson, B.G. Baldwin, Phylogenomics of Perityleae (Compositae) provides new insights into morphological and chromosomal evolution of the rock daisies. *J. Syst. Evol.*, 58(6), 853-880 (2020).
3. J.R. Mandel, R.B. Dikow, V.A. Funk, R.R. Masalia, S.E. Staton, A. Kozik, R.W. Michelmore, L.H. Rieseberg, J.M. Burke, A target enrichment method for gathering phylogenetic information from hundreds of loci: An example from the Compositae. *Applications in Plant Sciences*, 2(2), 1300085 (2014).
4. J.R. Mandel, M.S. Barker, R.J. Bayer, R.B. Dikow, T.G. Gao, K.E. Jones, S. Keeley, N. Kilian, H. Ma, C.M. Siniscalchi, A. Susanna, The Compositae tree of life in the age of phylogenomics. *J. Syst. Evol.*, 55(4), 405-410 (2017).
5. J.R. Mandel, R.B. Dikow, V.A. Funk, Using phylogenomics to resolve mega-families: An example from Compositae. *J. Syst. Evol.*, 53(5), 391-402 (2015).
6. A.M. Kozlov, D. Darriba, T. Flouri, B. Morel, A. Stamatakis, RAxML-NG: A fast, scalable and user-friendly tool for maximum likelihood phylogenetic inference. *Bioinformatics*, 35(21), 4453-4455 (2019).
7. A.J. Aberer, K. Kobert, A. Stamatakis, ExaBayes: Massively parallel Bayesian tree inference for the whole-genome era, *Mol. Biol. Evol.*, 31(10), 2553-2556 (2014).
8. C. Zhang, E. Sayyari, S. Mirarab, “ASTRAL-III: increased scalability and impacts of contracting low support branches.” In *RECOMB International Workshop on Comparative Genomics*, pp. 53-75, (Springer, Cham., 2017).
9. M. Dos Reis, P.C. Donoghue, Z. Yang, Bayesian molecular clock dating of species divergences in the genomics era. *Nat. Rev. Gen.*, 17(2), 71-80 (2017).
10. M. Dos Reis, J. Inoue, M. Hasegawa, R.J. Asher, P.C. Donoghue, Z. Yang, Phylogenomic datasets provide both precision and accuracy in estimating the timescale of placental mammal phylogeny. *Proc. Biol. Sci.*, 279(1742), 3491-3500 (2012).
11. A. Rambaut, A.J. Drummond, D. Xie, G. Baele, M.A. Suchard, Posterior summarization in Bayesian phylogenetics using Tracer 1.7. *Syst. Biol.*, 67(5), 901 (2018).
12. N.M. Koch, Phylogenetic subsampling and the search for phylogenetically reliable loci. *Mol. Biol. Evol.,* 38(9), 4025-4038 (2021).
13. S. Höhna, M.J. Landis, T.A. Heath, B. Boussau, N. Lartillot, B.R. Moore, J.P. Huelsenbeck, F. Ronquist, RevBayes: Bayesian phylogenetic inference using graphical models and an interactive model-specification language. *Syst. Biol.*, 65(4), 726-736 (2016).
14. E.E. Goldberg, B. Igić, On phylogenetic tests of irreversible evolution. *Evolution*, 62(11), 2727-2741 (2008).
15. B.G. Baldwin, B.L. Wessa, J.L. Panero, Nuclear rDNA evidence for major lineages of helenioid Heliantheae (Compositae). *Syst. Bot.*, 161-198 (2002).
16. M. Pagel, A. Meade, Bayesian analysis of correlated evolution of discrete characters by reversible-jump Markov chain Monte Carlo. *Am. Nat.*, *167*(6), 808-825 (2006).
17. M. Pagel, Detecting correlated evolution on phylogenies: A general method for the comparative analysis of discrete characters. *Proc. Biol. Sci.,* 255(1342), 37-45 (1994).
18. W. Xie, P.O. Lewis, Y. Fan, L. Kuo, M.H. Chen, Improving marginal likelihood estimation for Bayesian phylogenetic model selection. *Syst. Biol.*, 60(2), pp.150-160 (2011).
19. J. Rzedowski, *The vegetation of Mexico*. (Editorial Limusa, 1981).
20. J. McPhee, *Annals of the former world*. (Farrar, Straus and Giroux, 2000).
21. I.L. Wiggins, *Flora of Baja California*. (Stanford University Press, 1980).
22. J. P. Rebman, J. Gibson, K. Rich. Annotated checklist of the vascular plants of Baja California, Mexico. (San Diego Natural History Society, 2016).

23. Jepson Flora Project (eds.), *Jepson eflora,* https://ucjeps.berkeley.edu/eflora [accessed on Jul 01, 2021].
24. R.H. Ree, S.A. Smith, Maximum likelihood inference of geographic range evolution by dispersal, local extinction, and cladogenesis. *Syst. Biol.*, 57(1), 4-14 (2008).
25. K.A. Massana, J.M. Beaulieu, N.J. Matzke, B.C., O'Meara, Non-null effects of the null range in biogeographic models: Exploring parameter estimation in the DEC model. *bioRxiv* [preprint] (2015). https://www.biorxiv.org/content/10.1101/026914v1 (accessed 29 April 2021).
26. R.H. Ree, I. Sanmartín, Conceptual and statistical problems with the DEC+ J model of founder-event speciation and its comparison with DEC via model selection. *J. Biogeogr.*, 45(4), 741-749 (2018).
27. C.M. Tribble, W.A. Freyman, J.Y. Lim, M.J. Landis, J. Barido-Sottani, B.T. Kopperud, S. Höhna, M.R. May, RevGadgets: An R Package for visualizing Bayesian phylogenetic analyses from RevBayes. *Methods Ecol. Evol.*, *13*(2), pp.314-323 (2022).
28. Lichter Marck, I.H., and Baldwin, B.G., A phylogenetically informed reclassification of Perityleae. Syst. Bot. 47(2): in press (2022).
29. P. Carrillo-Reyes, A new species of *Perityle* (Asteraceae, Perityleae) from western Mexico. *Syst. Bot.*, 33(2), 459-461 (2008).
30. D.I. Axelrod, Edaphic aridity as a factor in angiosperm evolution. *Am. Nat.*, 106(949), 311-320 (1972).
31. A.H. Miller, J.T., Stroud, Novel tests of the key innovation hypothesis: Adhesive toepads in arboreal lizards. *Syst. Biol.*, *71*(1), 139-152 (2022).
32. I.H. Lichter-Marck, Plant evolution on bare rocky outcrops and cliffs: contrasting patterns of diversification following edaphic specialization. *aRxiv* [Preprint] (2022). https://arxiv.org/abs/2210.02880, (accessed: 24 November 2022).
33. M.J. Landis, W.A. Freyman, B.G. Baldwin, Retracing the Hawaiian silversword radiation despite phylogenetic, biogeographic, and paleogeographic uncertainty. *Evolution*, 72(11), 2343-2359 (2018).
34. K. Katoh, G. Asimenos, H. Toh, "Multiple alignment of DNA sequences with MAFFT." In *Bioinformatics for DNA sequence analysis*, D. Posada, Ed., pp. 39-64, (Humana Press, 2009).